Supporting Information

Bilayer-favored intercalation induced efficient and selective liquid phase production of bilayer graphene

Huiyong Wang,[1] Qiang Wan,[1] Zhansheng Lu,[2] Yanlei Wang,[3] Gaopeng Jiang,[4] Jie Shen,[5] Qiaochu Zeng,[5] Suojiang Zhang,[3] Zhongwei Chen[4]*, Jianji Wang[1]*

[1] Henan Key Laboratory of Green Chemistry, Collaborative Innovation Center of Henan Province for Green Manufacturing of Fine Chemicals, Key Laboratory of Green Chemical Media and Reactions, Ministry of Education, School of Chemistry and Chemical Engineering, Henan Normal University, Xinxiang, Henan 453007, P. R. China

[2] School of Physics, Henan Normal University, Xinxiang, Henan 453007, P. R. China

[3] Beijing Key Laboratory of Ionic Liquids Clean Process, Institute of Process Engineering, Chinese Academy of Sciences, Beijing 100190, P. R. China

[4] Department of Chemical Engineering, Waterloo Institute of Nanotechnology, University of Waterloo, 200 University Avenue West, Waterloo, ON N2L 3G1, Canada.

[5] Beijing National Laboratory for Condensed Matter Physics, Institute of Physics, Chinese Academy of Sciences, Beijing 100190, P. R. China

* zhwchen@uwaterloo.ca; jwang@htu.cn.

Table of Contents

1. Experimental procedures for the preparation of GICs and graphene

As a tri-component reaction at room temperature, both the amount of each component and the reaction time play important roles in the preparation of graphite intercalation compounds (GICs). To optimize the reaction condition, we used different consumption of CrO_3, HCl and reaction time from orthogonal design by keeping the amount of graphite to be constant (0.1g). Five levels were set for each factor, and the following orthogonal table was used for the three factors. Here, A, B, and C were applied to stand for time, amount of CrO_3, and that of HCl, respectively, and the subscript of each component stands for different levels.

Table S1. The orthogonal factor table for the optimization of preparation conditions of GICs

Factor Level	Time (h) A	CrO_3 (mol) B	HCl (mol) C
1	0.5	0.004	0.008
2	1.0	0.008	0.012
3	1.5	0. 015	0.016
4	2.0	0.016	0.020
5	2.5	0.020	0.024

If a compound is completely intercalated the interlayer galleries of graphite, ordered structures of the galleries will be significantly reduced, and thus result in the negative shift of the characteristic peak of 26.6° in XRD patterns. If the intercalation is incomplete and a part of graphite structure is still retained, an intensity-reduced graphite peak at 26.6 ° may be observed in XRD patterns. What is more, a new sharper peak indicates the better crystalinity of GIC. Therefore, XRD spectroscopy is a useful tool to evaluate the intercalation efficiency in the preparation of GICs.

The XRD patterns of GICs prepared at different reaction time and different consumption of CrO_3 and HCl were presented in Figure S1. It was found that with the increase of reaction time, the intensity of the peak at 26.6 ° was reduced, and this peak was disappered up to 2.5 hours. This result indicates that the ordered structure of graphite was completely converted to GIC after 2.5 hours. In addition, when the mole number of CrO_3 was equal to or greater than that of HCl, the peak at 26.6 ° became very weaken or even disappeared. Based on the above results, the optimized reaction condition was found to be 2.5 h, 0.016 mol of CrO_3 and 0.016 mol of HCl ($A_5B_4C_3$).

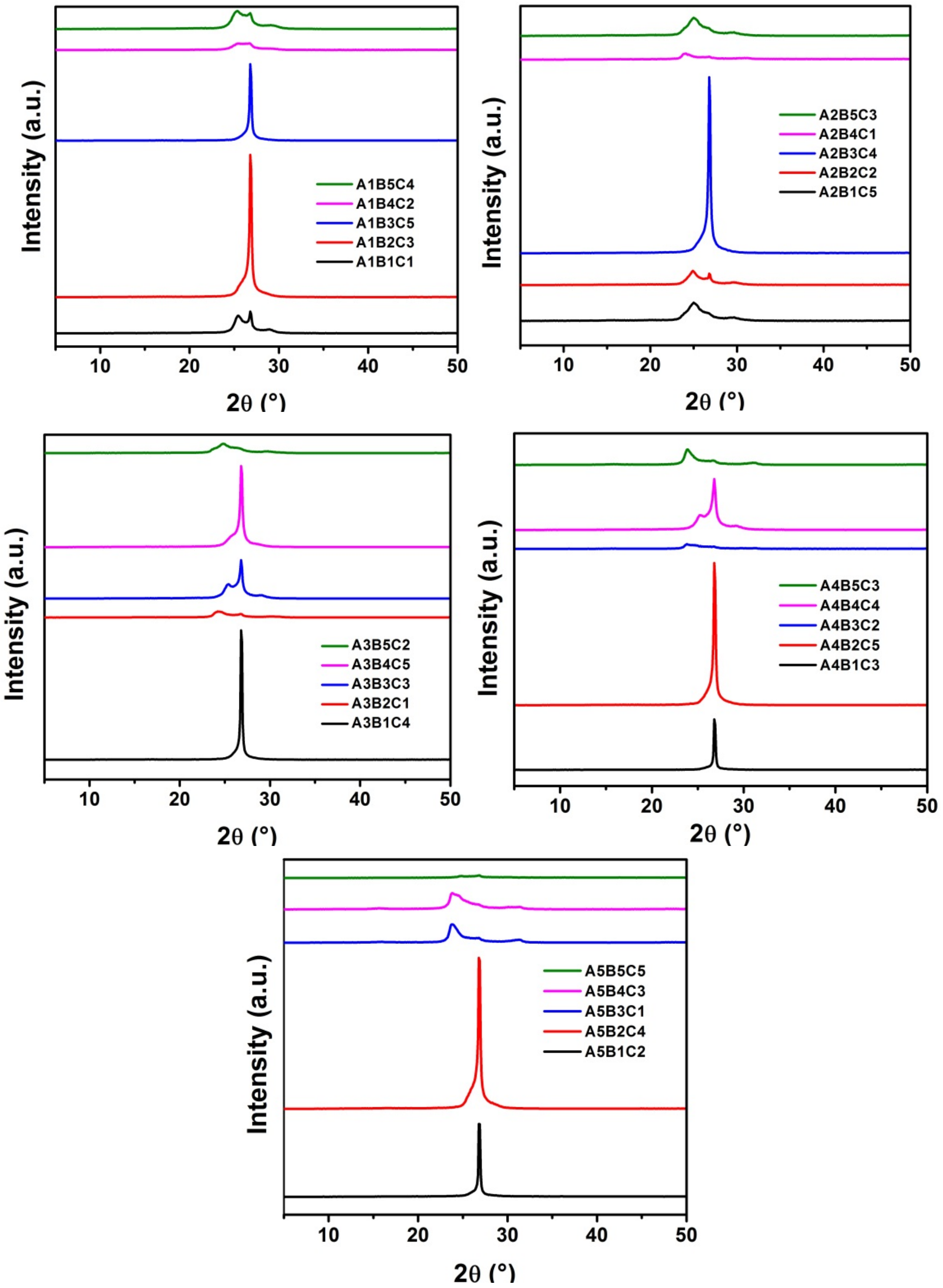

Fig. S1 XRD patterns of GICs prepared at different experimental conditions

The ratio of CrO_3: HCl is 1:1 and the mybe reason is following

Prior to the intercalation, CrO_2Cl_2 is formed through the following reaction of CrO_3 with HCl.

$$CrO_3 + 2HCl = CrO_2Cl_2 + H_2O \qquad (S1)$$

When HCl is excessive, then CrO_3 may further oxidize HCl into Cl_2 and form $CrCl_3$ and H_2O at the same time according to the following reaction:

$$2CrO_3 + 12HCl = 2CrCl_3 + 6H_2O + 3Cl_2 \qquad (S2)$$

Therefore, HCl cannot be excessive and the ratio of CrO_3: HCl should be at least 1:2 to guarantee the generation of CrO_2Cl_2. Actually, during the preparation of GIC, the concentrated hydrochloric acid (37 wt.% HCl) was used instead of anhydrous HCl gas. In this case, the water molecules in HCl solution can react with CrO_2Cl_2 and convert it into chromic and hydrochloric acid (reaction S3).

$$CrO_2Cl_2 + 2H_2O = H_2CrO_4 + 2HCl \qquad (S3)$$

This results in the decrease CrO_2Cl_2 concentration in solution and hence leads to no formation of GIC. Therefore, to ensure the enough concentration of chromoyl chloride, CrO_3 should be excessive and a ratio of 1:1 of HCl : CrO_3 was carried out in this work. It was found that 1:1 molar ratio of HCl : CrO_3 is suitable to the formation of stage-two GIC. These sentences have been added in the revised Supporting information.

2. X-ray diffraction patterns and SEM images of the starting graphite, stage-two GICs and expanded graphite

As shown in Fig. S2a, the starting graphite only exhibits one characteristic peak at 26.6° with relatively high diffraction intensity due to the good order along c-axis direction. If the intercalation was incomplete and part of the graphite structure was still retained, an intensity-reduced graphite peak can be observed. However, if no graphite structure was retained in GICs, only GICs peaks would be observed. As shown in Fig. S2b, three adjacent characteristic diffraction peak (15.4, 23.6, 31.2°) rather than the graphite peak (26.6°) were visible, from which a stage-two intercalation structure was determined definitely.

In addition, it can be seen that the intensity of these diffraction peaks decreased by more than 2 orders of magnitude relative to the graphite diffraction peak due to the increased interlayer distance. After expansion, expansion graphite showed a further decreased diffraction intensity, as shown in Fig. S2c, where the graphite diffraction peak (26.6°) was very weak because of the further decreased interlayer structural homogeneity.

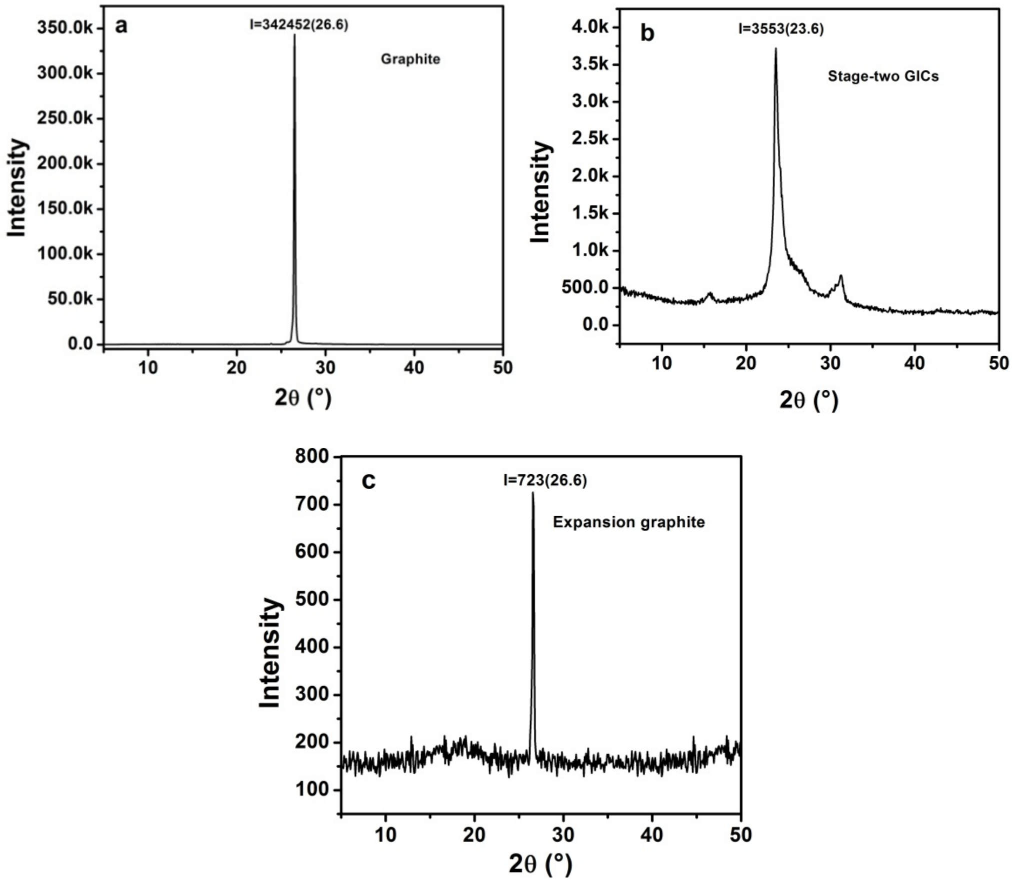

Fig. S2 XRD patterns of the starting graphite, stage-two GICs and expansion graphite.

As illustrated in Fig. S3, the intercalation of compounds into graphite (flake size for 325mesh) led to an increase in average thickness of graphite flakes, changing from 0.55 ± 0.1 μm to 1.63 ± 0.26μm. After liquid-phase expansion of GICs, the GICs are changed into CEGs and the average thickness of CEGs is 156 ± 27 μm. Then, the mean expansion ratio is calculated as the ratio of the mean thickness of CEG over that of graphite.

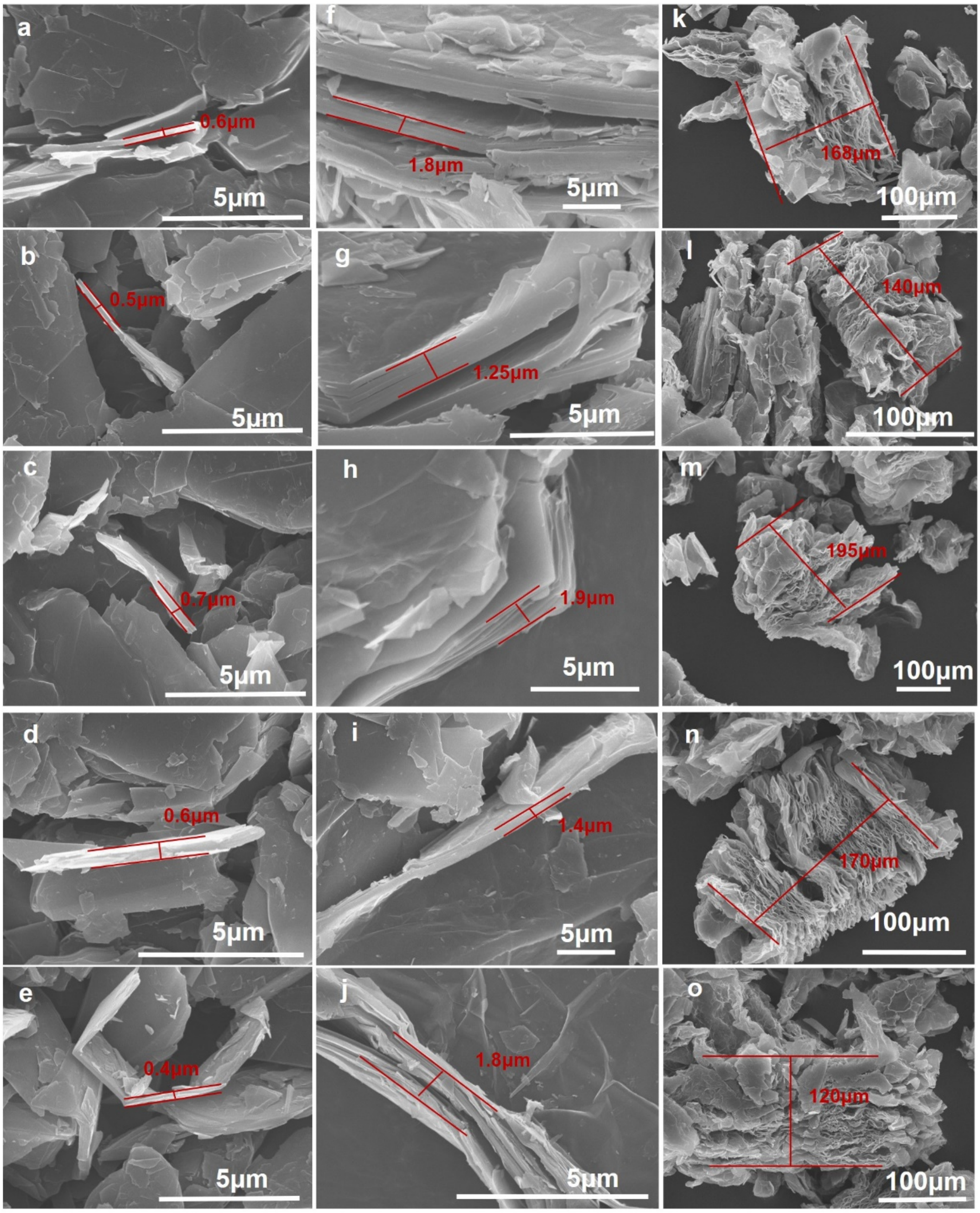

Fig. S3 SEM images of graphite (a-e), GIC (f-j) and CEG (k-o).

3. The effect of crystallinity and particle size of graphite on the GIC structures

As the crystallinity and particle size of graphite play an important role in intercalation reaction, pristine graphite materials with different sizes (an average size of 100, 325, and 800 mesh) were used to prepare GICs. The resultant GICs were characterized by X-ray diffraction (XRD). It was found that both the XRD pattern and Raman spectra of GIC prepared by 800 mesh of pristine graphite were similar to those prepared by 325 mesh of pristine graphite (Fig. S4 and Fig. S5). This indicates that 800 mesh of pristine graphite could be transferred into stage-two GICs. However, the resulting graphene was seriously oxidized as evidenced from a high intensity ratio of D and G peaks (I_D/I_G, 0.48) of the graphene in Raman spectrum (Fig. S6) as well as the high oxygen content of 10.6% from XPS (Fig. S7). The main reason is that the pristine graphite with larger mesh has small size, which results in the easier interaction reaction and the resulting graphene is oxidized more easily. On the other hand, GIC powders prepared from 100 mesh of pristine graphite was stage-three GICs, as reflected by XRD and Raman spectra. The four adjacent diffraction peaks (30.4, 26.6, 24.3, 18.3^o)[1] and a 26.6^o peak of the pristine graphite were observed in the GIC powders prepared from 100 mesh of pristine graphite, which means the GIC was stage-three GIC and an inefficient intercalation of the compound into graphite was existed due to the larger size of the pristine graphite. The G peak of this GIC splits into two peaks with the major peak upshifted by about 20 cm^{-1} indicates the presence of stage-three or upwards compounds.[2]

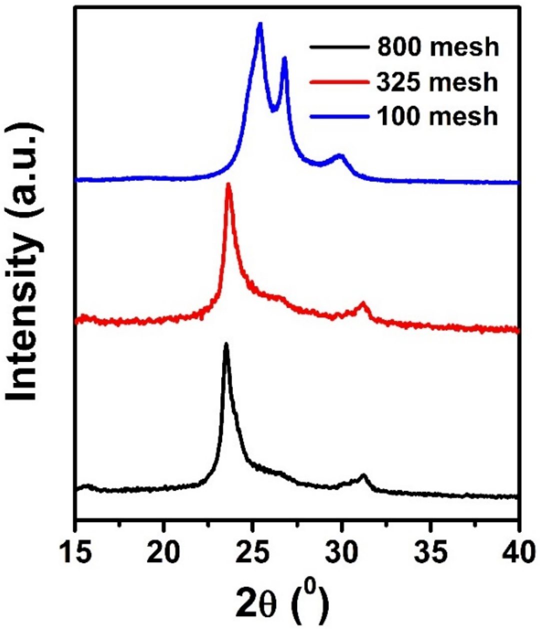

Fig. S4 XRD patterns of GICs prepared by starting graphite with different meshes.

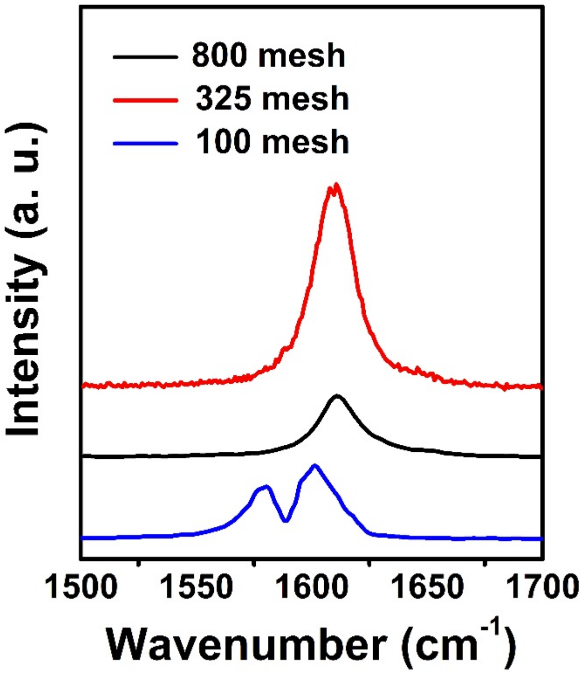

Fig. S5 Raman spectra of GICs prepared by starting graphite with different meshes.

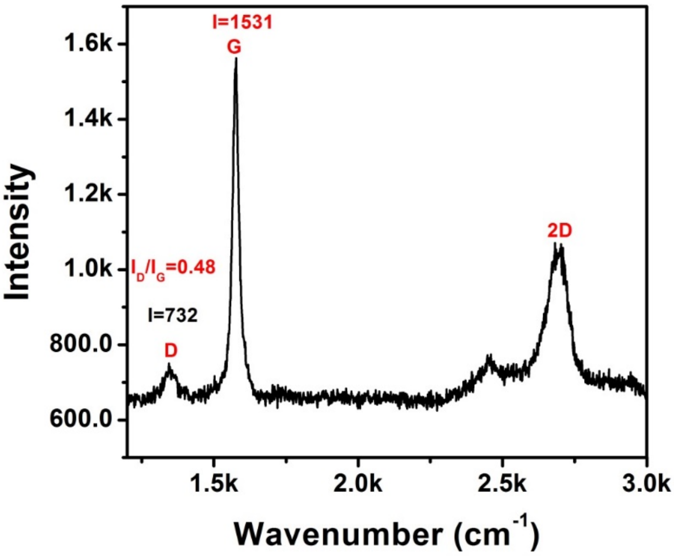

Fig. S6 Raman spectrum of the graphene obtained from pristine graphite with 800 mesh.

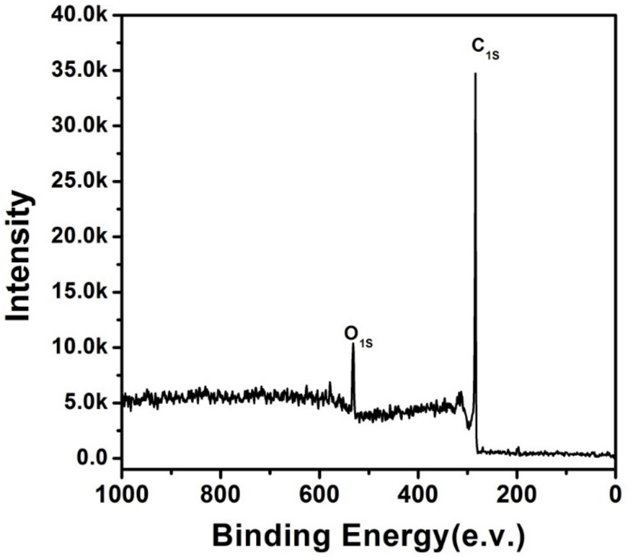

Fig. S7 XPS survey of graphene obtained from starting graphite with 800 mesh.

4. Calculation of yield and selectivity of the bilayer graphene

A certain amount of as prepared graphene is dispersed onto the h-BN base and then these graphene flakes are observed by AFM. Assuming that the area of each graphene flake with L layers is $A_{L,i}$, the mass of this graphene ($m_{L,i}$) can be estimated as

$$m_{L,i} = d_A \times A_{L,i} \times L \tag{S4}$$

where d_A is the areal density of single layer graphene and is 0.77 mg/m^2. Therefore, the total mass (m_L) of n pieces of graphene with L layers was calculated by the following equation:

$$m_L = \sum_i^n m_{L,i} = \sum_i^n d_A \times A_{L,i} \times L = d_A L \sum_i^n A_{L,i} \tag{S5}$$

The weight percentage of bilayer graphene was computed by this equation:

$$m_2\% = \frac{m_2}{\sum_L^N m_L} = \frac{2\, d_A \sum_i^n A_{2,i}}{d_A \sum_L^N \left(L \sum_i^n A_{L,i} \right)} = \frac{2 \sum_i^n A_{2,i}}{\sum_L^N \left(L \sum_i^n A_{L,i} \right)} \tag{S6}$$

The yield ($W_2\%$) of BLG was calculated by this equation:

$W_2\%= m_2\% \times (M_{graphene}/M_{graphite})$ (S7)

In this equation, $M_{graphene}$ and $M_{graphite}$ stand for the total mass of obtained graphene and mass of input graphite, respectively.

In order to clearly understand this calculation method, an example of a computational process is given below. In this AFM image, the graphene sheets marked with the flakes 1, 2-13, 14 are SLGs, BLGs, and tri-layer graphene, respectively. The area of each sheet is computed based on the computer image processing technology.

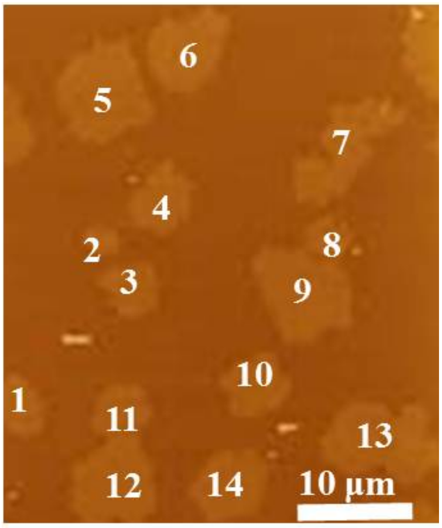

According to the equation S5, the weight of SLG is calculated as follows:

$$m_1 = 1 \times d_A \sum_{1}^{1} A_{1,1} = 0.77 mg/m2 \times 1 \times 20.3 \mu m2 = 15.63 \times 10^{-6}\ \text{mg}$$

Likewise, the weight of BLG is calculated:

$$m_2 = 2 \times d_A \sum_{1}^{12} A_{2,1} = 0.77\ mg/m2 \times 2 \times (8.3 + 12.2 + 20.1 + 30.1 + 24.8 + 3$$

$$+ 8.6 + 49.3 + 20.6 + 11.6$$

$$+ 43.2 + 47.8) \mu m2$$

$$= 480.79 \times 10^{-6}\ \text{mg}$$

Then, the weight of graphene with triple layer is calculated:

$$m_3 = 3 \times d_A \sum_{1}^{1} A_{3,1} = 0.77\ mg/m2 \times 3 \times 26.7\ \mu m2$$

$$= 61.68 \times 10^{-6}\ \text{mg}$$

Finally, the weight percentage of BLG is calculated:

$$m_2\% = \frac{m_2}{\sum_{L}^{N} m_L} = \frac{m2}{m1 + m2 + m3} = \frac{480.79}{15.63 + 480.79 + 61.68} = 86.1\%$$

After statistics and analysis, the yield ($W_2\%$) of BLG was obtained according to the equation (S7)

$$W_2\% = 81.85\% \times (0.658\text{g}/1.03\text{g}) = 52.3\%$$

Selectivity = number of the bilayer graphene pieces divided by total number of the graphene pieces determined from all AFM images: 122/141=86.5%

5. The characterization of BLG obtained from starting graphite with 325 mesh

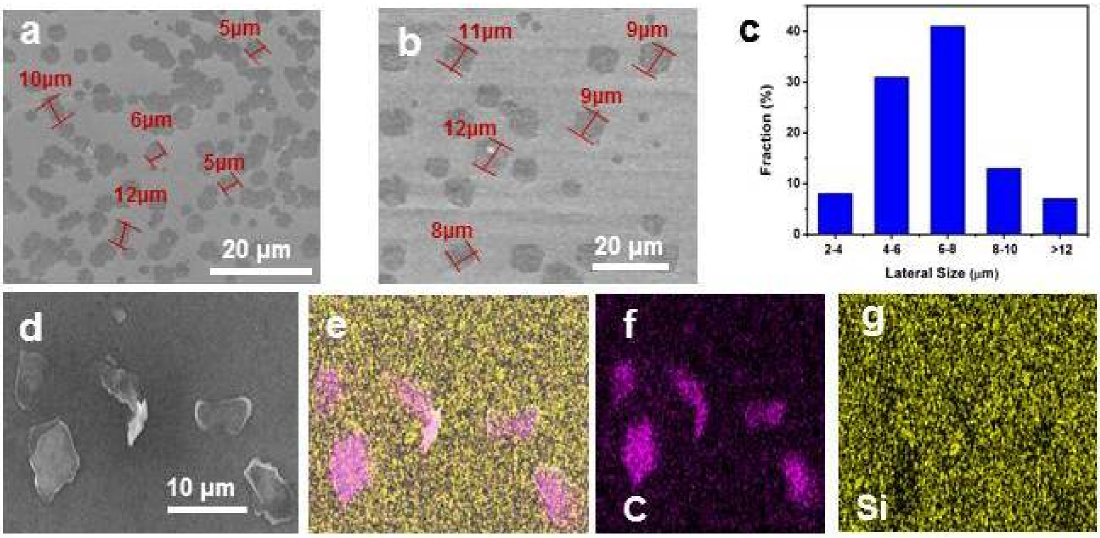

Fig. S8 SEM images (a-b, d) of the graphene sheets obtained from starting graphite with 325 mesh at arbitrarily selected area and their lateral size distribution calculated from 120 sheets (c), the element distribution of graphene (e-g) revealed by element mapping, indicating the carbonaceous nature of BLG nanosheets.

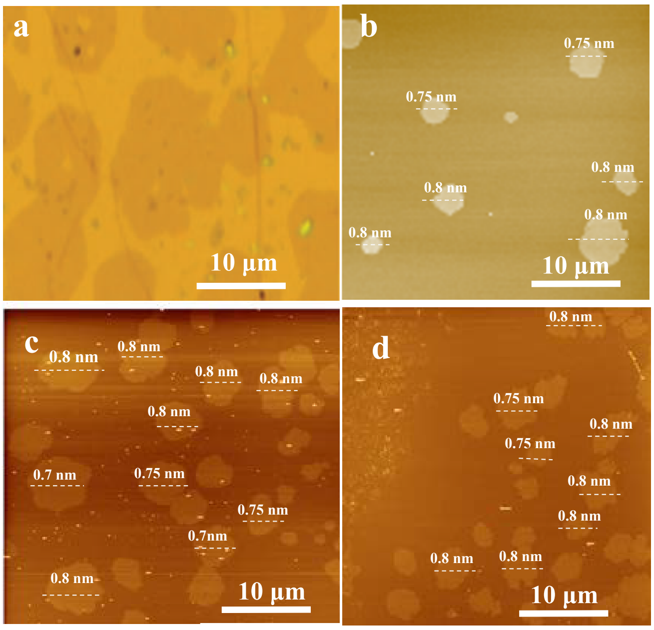

Fig. S9 AFM images of the graphene sheets obtained from starting graphite with 325 mesh.

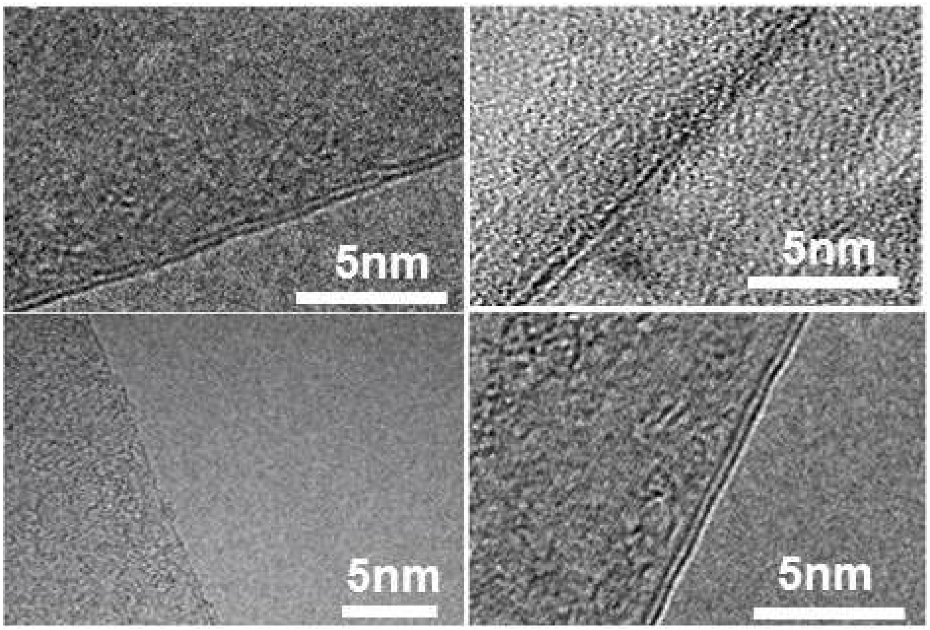

Fig. S10 HR-TEM image of edge structure of the bilayer graphene sheets obtained from starting graphite with 325 mesh.

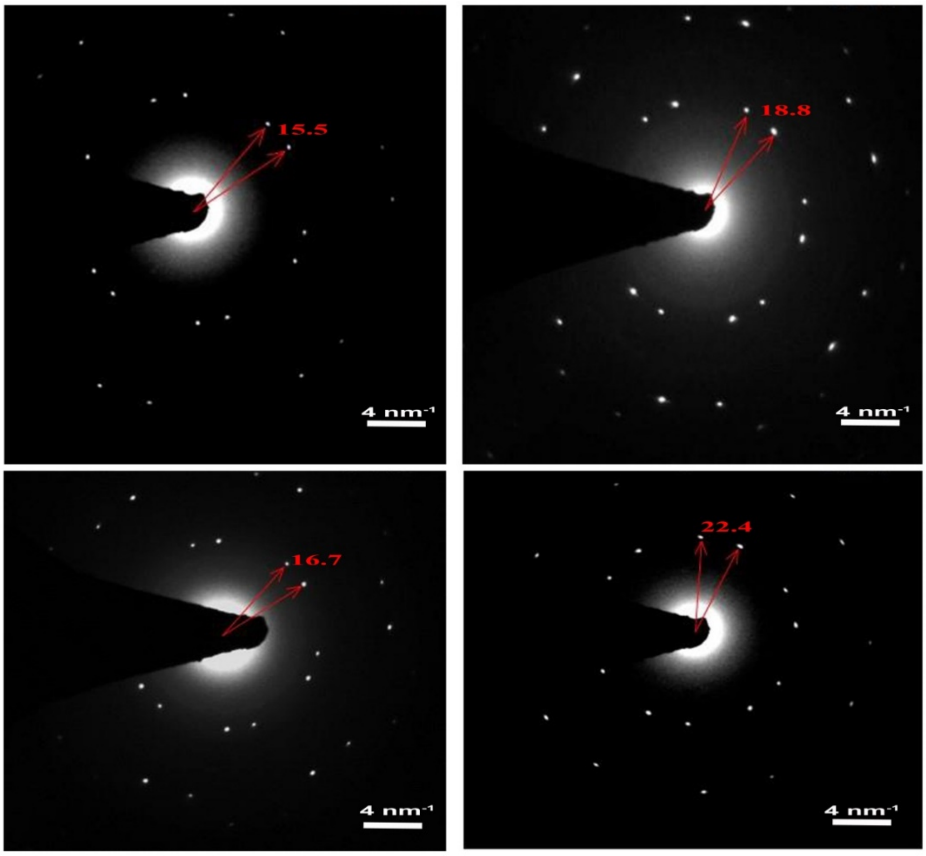

Fig. S11 The twist angle of graphene sheets obtained from starting graphite with 325 mesh.

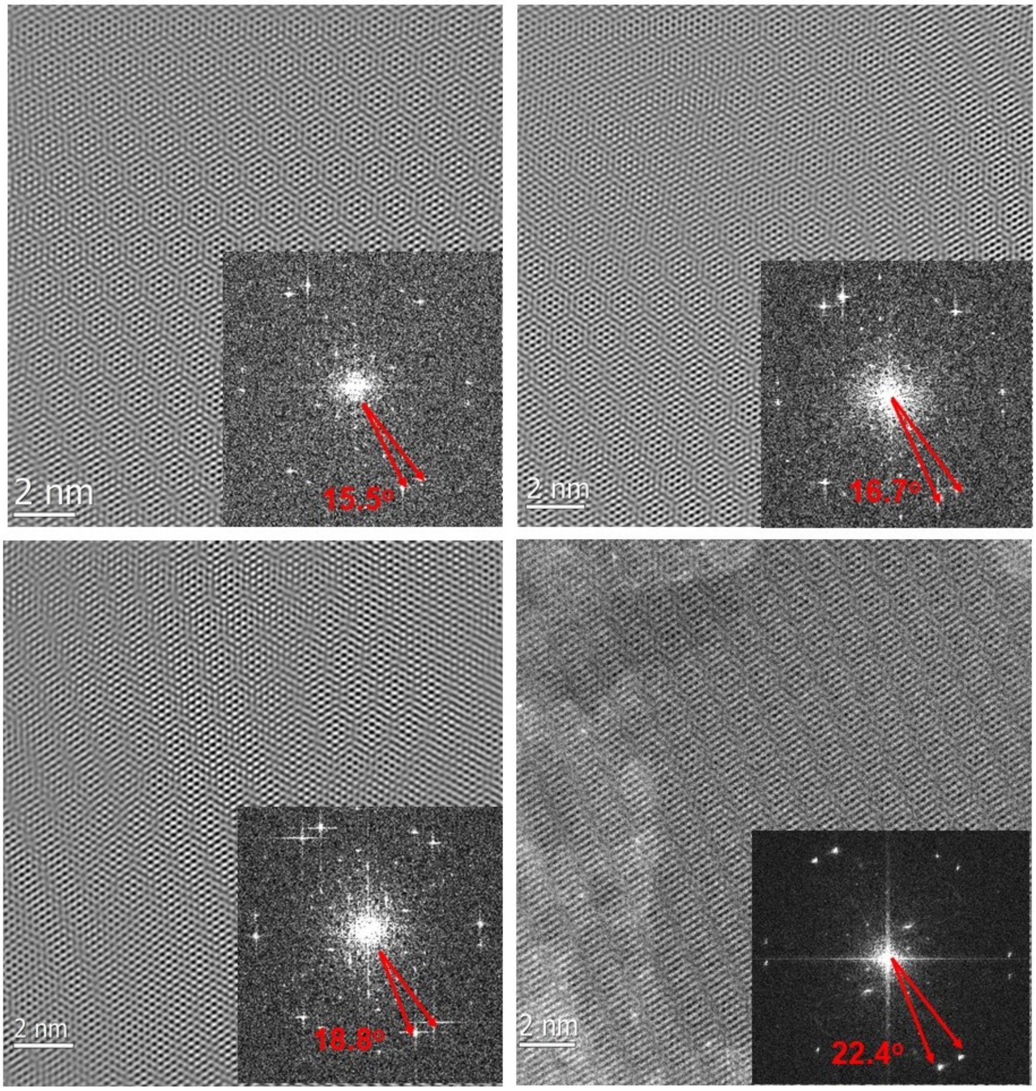

Fig. S12 The Moiré pattern of ADF-STM images of bilayer graphene with different twisted angle (Inset shows a fast Fourier transform (FFT) of the image.

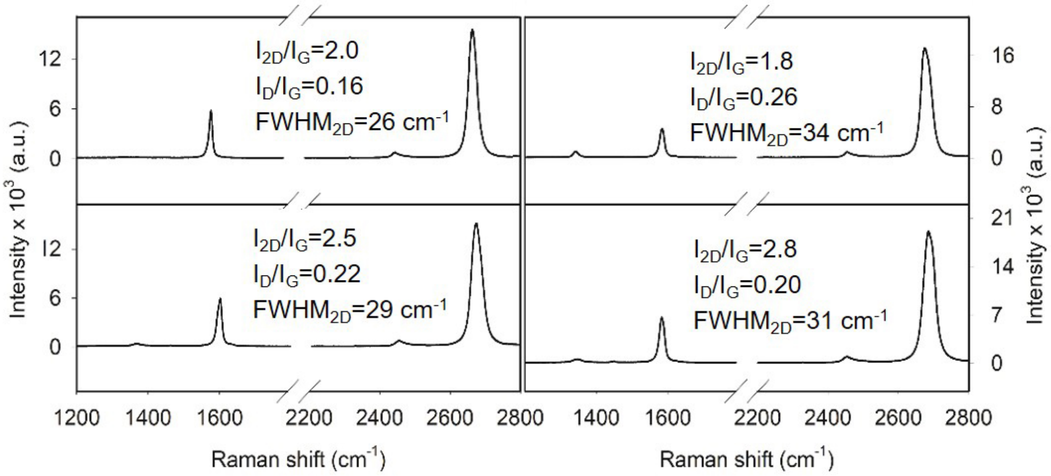

Fig. S13 Raman spectra of the resultant graphene.

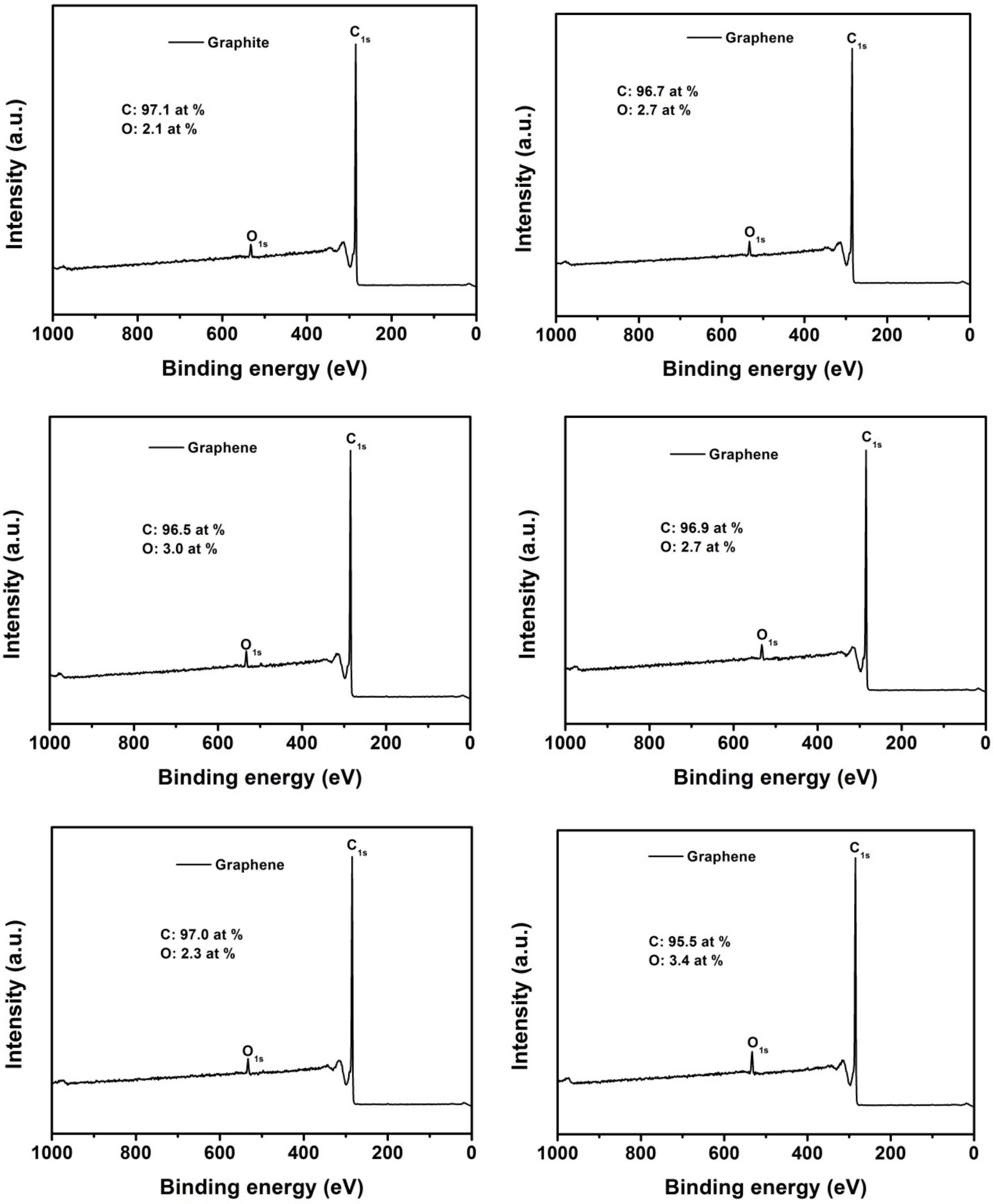

Fig. S14 XPS survey of the starting graphite (325 mesh) and the resultant graphene.

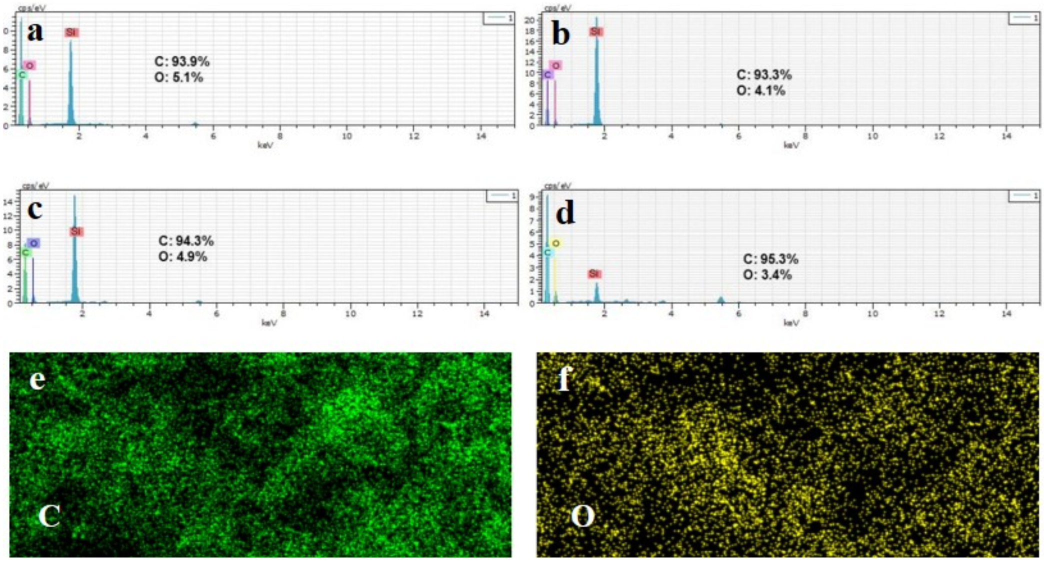

Fig. S15 The content of C and O element (a-d) and their mapping distribution (e-f) in the graphene deposited on a Si substrate.

6. The XPS spectrum of stage-two GIC

The XPS spectrum was also carried out on the stage-two GIC to determine the intercalating species. In the Cr 2p X-ray photoelectron spectrum (Figure S16), the four peaks at binding energies of 579.0, 588.3, 577.0, and 586eV observed were due to $2p_{3/2}$, $2p_{1/2}$ electrons of Cr^{6+}, and $2p_{3/2}$, $2p_{1/2}$ electrons of Cr^{3+}, respectively.[3] However, the total amount of Cr^{3+} was very small, compared with Cr^{6+}. Therefore, the species intercalated into graphite should contain a lot of Cr^{6+} compounds and a tiny amount of Cr^{3+}.

The O ls spectra in Figure S17 showed the presence of four kinds of oxygen on the surface of the GIC. The peak at binding energy 530.2eV may be ascribed to oxygen attached to Cr (Cr=O). [3] The other three peaks at binding energies of 532.0, 533.1 and 534.3 eV were ascribed to oxygen attached to carbon. Peaks between binding energies of 196 and 203 eV in the XPS spectrum showed the presence of chlorine in the GIC (Figure S18). The binding energies of 198.2 and 199.8 eV may be attributed to the $2p_{3/2}$ and $2p_{1/2}$ electrons of ionic chlorine (Cl^-) in the GIC. At higher binding energies of 200.2 ($2p_{3/2}$) and 201.8 ($2p_{1/2}$) eV may be ascribed to the chlorine attached to chromium (Cr-Cl).[3] These results also indicated that the CrO_2Cl_2 existed in the stage-two GIC as intercalating species, which was in line with the results from infrared spectra.

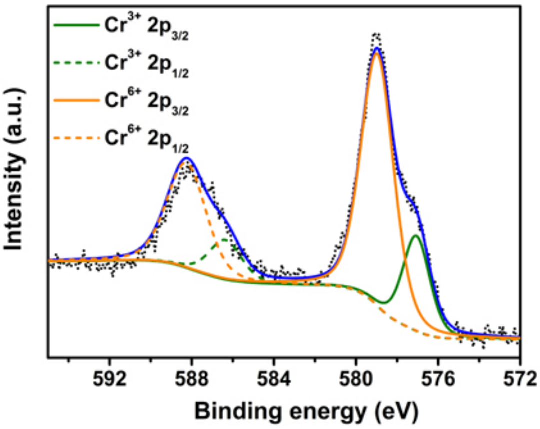

Fig. S16 The high-resolution Cr 2p spectra of stage-two GIC

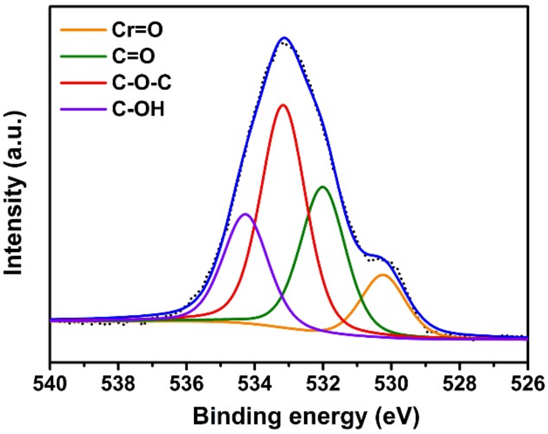

Fig. S17 The high-resolution O 1s spectra of stage-two GIC

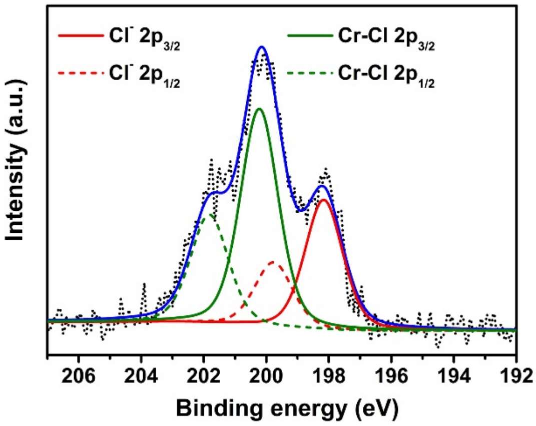

Fig. S18 The high-resolution Cl 2p spectra of stage-two GIC

7. Tables S2-S5

Table S2 The concentration of exfoliated graphene in different solvents

Solvents	Concentration(mg ml^{-1})
Water	0.01
DMPA	3.0
Dimethyl sulfoxide	0.1
N-methyl-2-pyrrolidone	0.8
N,N-dimethylformamide	0.2
Ethanol	0.06
Isopropanol	0.3

Table S3 The comparison of the methods for the preparation of bilayer graphene sheets

Method	Comments	Yield	Lateral size/ areas	I_D/I_G	C/O	Ref
Epitaxial formation of bilayer Bernal graphene on copper foil via chemical vapor deposition at 1000 °C	High energy consumption	-	50 μm	D peak negligible	-	4
Copper-catalysed low-pressure CVD using a gas mixture of Ar, H_2 and diluted CH_4	High energy consumption	-	300 μm	No D peak	-	5
ICl-intercation highly-ordered pyrolytic graphite at 160 °C for 24 hours, expansion at 800 °C and sonication exfoliation	High energy consumption	3%	50μm^2	~0.15	-	6
Room-temperature intercalation of CrO_3 and mild sonication exfoliation		52.3%	4~8 μm	0.12	37	This work

Table S4 The average content of C and O element, and corresponding ratio of C/O in BLG determined by XPS and EDX

Methods	C	O	C/O
XPS	96.6±0.6 at %	2.7±0.5 at %	37±7
EDX	94.2±0.8 at %	4.4±0.8 at %	22±4

Table S5 The comparison of field-effect mobility of BLG with high quality

Method	Mobility (cm^{2}V^{-1}s^{-1})	Ref.
CVD	8000	ACS Nano, 2013, 7, 2587
CVD	8117	Nat. Commun., 2013, 4, 2096
CVD	7600	Phys. Rev. B, 2012, 85, 201408(R)
Micromechanical cleavage	3000~8000	Phys. Rev. Lett., 2008, 100, 016602
Liquid phase exfoliation	6900	This work

References

1 M. Matsumoto, Y. Saito, C. Park, T. Fukushima, T. Aida, *Nat. Chem.*, 2015, **7**, 730-736.

2 C. Underhill, S. Y. Leung, C. Dresseihaus and M. S. Dresselhaus, *Solid State Commun.*, 1979, **29**, 769-774, https://doi.org/10.1016/0038-1098(79)90158-3.

3 C. D. Wanger, In Practical Surface analysis, D. Briggs, M.P. Seah, ed. (Wiley New York), pp. 595 (1990).

4 K. Yan, H. Peng, Y. Zhou, H. Li and Z. Liu, *Nano Lett.*, 2011, **11**, 1106-1110.

5 H. Zhou, W. J. Yu, L. Liu, R. Cheng, Y. Chen, X. Huang, Y. Liu, Y. Wang, Y. Huang and X. Duan, *Nat. Commun.*, 2013, **4**, 2096.

6 C. J. Shih, A. Vijayaraghavan, R. Krishnan, R. Sharma, J. H. Han, M. H. Ham, Z. Jin, S. Lin, G. L. Paulus, N. F. Reuel, Q. H. Wang, D. Blankschtein, M. S. Strano, *Nat. Nanotechnol.*, 2011, **6**, 439-445.